The Diameter of Cortical Axons Depends Both on the Area of Origin and Target.

(Article begins on next page)

21 August 2024

OXFORD
UNIVERSITY PRESS

Cerebral Cortex

THE DIAMETER OF CORTICAL AXONS DEPENDS BOTH ON AREA OF ORIGIN AND TARGET

THE DIAMETER OF CORTICAL AXONS DEPENDS BOTH ON AREA OF ORIGIN AND

TARGET

Giorgio M Innocenti[1], Alessandro Vercelli[2] and Roberto Caminiti[3]

1. Department of Neuroscience, Karolinska Institutet, Stockholm, Sweden;

2. Neuroscience Institute of the Cavalieri Ottolenghi (NICO), Department of Neuroscience,

    University of Turin, Turin, Italy;

3. Department of Physiology and Pharmacology, University of Rome Sapienza, Rome, Italy.

Corresponding author:

Giorgio M Innocenti, Department of Neuroscience Karolinska Institutet, Retzius väg 8, S17177

Stockholm, Sweden

Phone: +46852487862

Mob: +46704681536

E mail: Giorgio.Innocenti@ki.se

Running title: Diameter of cortical axons

ABSTRACT

In primates, different cortical areas send axons of different diameter into comparable tracts, notably the corpus callosum (Tomasi et al. 2012). We now explored if an area also sends axons of different diameter to different targets. We find that the parietal area PEc sends thicker axons to area 4 and 6, thinner ones to the cingulate region (area 24). Areas 4 and 9, each sends axons of different diameter to the nucleus caudatus, to different levels of the internal capsule, and to thalamus. The internal capsule receives the thickest axon, followed by thalamus and nucleus caudatus. The two areas (4 and 9) differ in the diameter and length of axons to corresponding targets. We calculated how diameter determines conduction velocity of the axons and together with pathway length determines transmission delays between different brain sites. We propose that projections from and within cerebral cortex consist of a complex system of lines of communication with different geometrical and time computing properties.

Key words: conduction velocity, cortical area, internal capsule, nucleus caudatus, thalamus

Axons originating in different cortical areas of the macaque monkey differ in their diameter, with thickest axons originating in primary motor and somatosensory areas and the thinnest ones in prefrontal and temporal areas (Tomasi et al. 2012). Areal differences in axon diameter were found for callosal axons and for cortico-thalamic axons, but not for intra-area axons. The diameter of outgoing axons, therefore, appears to be a feature characterizing cortical areas, in addition to the classical size and distribution of cell bodies, degree of myelination, topography of connections, neuronal response properties, etc. Axon diameter determines conduction velocity and together with axon length generates temporal delays whereby different brain sites communicate. It was proposed that conduction delays may constrain processing speed and that there may be a hierarchy of processing speeds among cortical areas, with premotor, motor and primary somatosensory areas on the lead (Tomasi et al. 2012). Areas with, on average, thicker axons also had an increased spectrum of axon diameters and of conduction delays. These differences appear to be exaggerated in evolution in parallel with the increased volume of the brain and might enrich cortical dynamics (Caminiti et al. 2009).

It was unclear if diameter relates only to the area of origin of the axons or also to their sites of termination. This question was tackled in the present study by comparing the diameter of axons originating in posterior parietal cortex and terminating in motor, premotor and cingulate cortex. We also compared axons originating in area 4, and in prefrontal cortex area 9, and terminating in the caudate, and thalamus or continuing into the internal capsule.

Materials and Methods

Two monkey brains injected with biotinylated dextran amine (BDA) in the dorsal part of area 4, presumably the proximal arm/trunk representation, were at our disposal (Tomasi et al. 2012); one of them was also injected in prefrontal area 9. This allowed reducing the number of animals as much as possible since in studies with primates the repetition of experiments is restricted by ethical considerations and administrative rules; the projection from parietal cortex was studied in a third animal. An additional monkey injected in area PEc was prepared for electron microscopy (EM) and intracortical axons were measured in parietal cortex. The surgical methods were reported in detail in Tomasi et al. (2012). Briefly, deeply anaesthetized animals received three to five 0.3-0.5 µl injections of BDA (Invitrogen, Carlsbad, CA) MW 10 000 (10% in 0.01 M phosphate buffer) in area 4, 9 and PEc/PE border (area 5). The monkeys were males ranging between 6 and 8 years of age and weighing between 6 and 10 kg.

For EM, one animal was perfused 5 minutes with heparinized buffered saline followed by 2 Lt of 3% paraformaldehyde (PAF) and 1% glutaraldehyde in 0.9% NaCl in 0.15 M Phosphate Buffer (PB). The skull and the dura were opened and the head was stored in 3% PAF in 0.9% NaCl in 0.15 M overnight. The following day, the corpus callosum was cut on the midline. Parasagittal blocks were cut from each hemisphere, containing the injection site and the labeled fibers. 80 µm-thick sections were obtained at the vibratome and reacted for BDA according to Wang et al. (2010). Selected sections were osmicated and flat embedded in Araldite, to be sectioned for EM. Semithin sections were cut on the ultramicrotome with a glass knife, to outline the area of interest; ultrathin sections (from silver to gold) were cut with a diamond knife, counterstained with uranyl acetate and lead citrate, and observed with a JEM-1010 transmission electron microscope (JEOL, Tokyo, Japan) equipped with a Mega-View-III digital camera and a Soft-Imaging-System (SIS, Münster, Germany) for the computerized acquisition of the images,

at the magnification of 10k or 20k, for measuring myelinated and unmyelinated fibers, respectively. The diameter of BDA labeled axons identified in the gray matter near the injection site was measured in four different specimens, using the software ImageJ (NIH, USA) by drawing a line along the shortest axis of the axon profile. BDA-labeled axons were identified under the EM by the greater electron density of the cytoplasm, except for mitochondria, particularly in the vicinity of vesicular and other membranes.

For light microscopy (LM) sections from brains cryoprotected in 30% (wt/vol) sucrose in PBS were cut frozen at 34 μm and reacted for BDA with alternating sections stained for cresyl violet and the Gallyas method for myelin as in Tomasi et al. (2012).

Axons originating in area PEc/PE were sampled and measured as in Tomasi et al. (2012). The axons profiles at the upper or lower surface of the sections were approximated to circles whose size was incremented in 0.09 μm steps. Axons originating in areas 4 and 9 were sampled and measured with the following strategy using the Neurolucida software (MBF Biosciences, Williston, VT). Since each monkey had received injections at different locations a preliminary sketchy reconstruction of the pathway was performed at 345 x (2 cm=58 μm) magnification to separate the different projections. Areas of interest were circumscribed and within these areas 80-119 axon segments traversing the section were drawn at 3448 x magnification (2 cm=5.8 μm) over their entire length i.e. between 5 and 70 μm faithfully following the changes in diameter that the axon undergoes in its trajectory. The Neuroexplorer software (MBF Biosciences, Williston, VT) calculated the diameter of the axonal segment at the surface of the section as well as the average diameter of the axonal segment. The two types of measurements are similar but not identical. The average diameter can be affected by apparent thinning of the axon due to incomplete visualization in the depth of the section. The diameter of the axon at the surface of

the section more closely approximates the measurements performed with the circle and, as the latter, is affected by whether the section fell by chance on a thin or on a varicose portion of the axon. Eventually the latter measurement at the surface of the section was retained.

Significance of differences was tested with the Mann Whitney two-tailed U test.

Lengths of tracts were measured as curvilinear segments with one of the Neuroexplorer software options (MBF Biosciences, Williston, VT).

Correction for shrinkage. Shrinkage in this material consisted of two components. The first component is due to the perfusion–fixation and was estimated by comparing the distance between the sites of injection at the time of the stereotaxic measurements and on the sections in 4 animals. This component varied between 1.1 and 1.4 (mean 1.2). The second component is the differential shrinkage between the BDA and the cresyl violet or myelin staining. This component was negligible. Therefore we applied a 1.3 correction for shrinkage to the results on the distribution of axon diameters and conduction velocities of axons originating in area 4 in order to test if the shrinkage of the histological material might explain the differences between our anatomical results and some electrophysiological data in the literature (Discussion).

Results

Sites of Injection and Axonal Trajectories

The sites of injection are shown in Fig. 1. The core of the injections was between 500 μm and 2 mm in diameter, restricted to the gray matter. The location was based on cytoarchitectonic criteria and on comparisons with Paxinos et al. (2000) atlas. The axonal trajectories correspond to those reported by Schmahamann and Pandya (2009) for similar injection locations

(Discussion). They can also be appreciated in Figs 3 and 5 and therefore they will not be described in detail.

Electron Microscopic Analysis of Axon Diameters

The limited resolution of the LM could introduce biases in our assessment of axon diameters. For certain tracts, notably the corpus callosum, our estimates could be compared with EM data in the literature and this possible source of error could be avoided (discussed in Tomasi et al. 2012). Unfortunately, a comparison of our measurements with EM data is not available for all tracts and it is not feasible to analyze all the corticofugal tracts of the monkey with combined tract-tracing and EM techniques. In this study one monkey was injected with BDA in the PEc subdivision of area 5, and the diameter of the labeled local intra-cortical axons was measured in EM photomicrographs. The choice was dictated by two considerations. The first is that the local intra-cortical axons are likely to be the thinnest since many of them span much shorter distances than the other corticofugal axons. The second is that the diameter of local intra-cortical axons was found to be surprisingly similar in the five areas (9, 9/46, 6, 6-F4 and 4) where they were studied in three different animals (Tomasi et al. 2012). If a comparable spectrum of axon diameters were to be found in the new experiment, it could confirm that i) the LM analysis is not seriously biased by missing small axons and that ii) the intracortical axons are indeed of similar diameter across different cortical areas. Examples of BDA-labeled myelinated and unmyelinated axons are shown in Fig. 2. Sixty-six myelinated axons were measured. Their mean diameter was 0.76 μm (± 0.29, sd; median 0.71), of which the axoplasm was 0.53 μm (± 0.24, sd; median 0.49). The axoplasm/axon ratio was, as expected, almost exactly 0.7. Seventy-five unmyelinated axons were measured and their mean diameter was 0.44 μm (± 0.16, sd; median 0.4; marginally

smaller, P<0.05, than the axoplasm of the myelinated-axons). Since BDA appears not to diffuse into the myelin sheath, the comparison between EM and LM data was restricted to the axoplasm. The EM values we found for the axoplasm of BDA labeled axons falls within the range of intracortical axon diameters previously measured with LM (0.48-0.66 μm; Tomasi et al. 2012) and it is nearly identical to the axon diameters found in the same study (0.48-0.51 μm) in areas 9, 9/46, 6 and 6-F4 while those from area 4 were slightly thicker (0.54, 0.66 μm).

Cortico-cortical Projections from Area PEc

The cortico-cortical axons originating in area PEc (Fig. 3) course in the superior longitudinal fasciculus (SLF; subdivision SLF I of Schamahmann and Pandya, 2009). They terminated at three separate locations in areas 4, 24 and 6. In area 4, the axons ended in its caudal part, in three columns with the densest terminals in superficial layers, particularly in layer I. The projection is reciprocal since, in spite of the fact that the BDA used is transported overwhelmingly anterogradely, a few retrograde labeled neurons were seen in layer 3. In area 6, the axons ended on the convexity of the superior frontal gyrus in the dorso-caudal division of premotor cortex, cytoarchitectonically corresponding to area F2 of Belmalih et al. (2007). At the same rostrocaudal levels axons also terminated at the fundus and on the dorsal bank of the cingulate sulcus. This site of termination is cytoarchitectonically different from the more dorsal area 6m of Paxinos et al. (2000) (F3, according to Belmalih et al. 2007). The difference is the disappearance of large pyramids in layer 5, replaced by a band of medium size pyramids in layers 3 and 5 which therefore cannot be differentiated, also due to the absence of layer 4. This area of termination is characterized by a superficial band of tangentially coursing, myelinated axons which acquire a deeper location and lose their identity in the more dorsal cortex. The

termination corresponds to a subdivision of area 24 in the proximity to the fundus of the sulcus but it extends more dorsally ~~than what could be expected from the published boundaries of this area~~ and might reach area 6/32 according to Paxinos et al. (2000). At roughly corresponding locations Picard and Strick (1996) described cingulate motor areas, notably CMAd. ~~It will be referred to as area 24 in the rest of this paper.~~

Axons were measured in the SLF I before they distribute to their sites of termination and then at their entrance into the gray matter (Table 1 and Figs 3 and 4). Axons in the SLF were 1.03 µm on average (median 0.8). Those to areas 4 and 6 had similar diameters (means 0.95 and 0.96 µm; medians 0.8 and 0.87, respectively) while those to area 24 were thinner (mean 0.77 µm, median 0.73). Mann Whitney U test reported highly significant differences ($P<0.001$) between the axons to area 6 and those to area 24, marginally not significant differences ($P=<0.05$) for the other comparisons.

The axons labeled by the BDA injection in area PEc were a subpopulation of the myelin-stained SLF axons. Profiles of cross-sectioned myelinated axons were sampled in SLF (10921; preliminary work for another study). Their average near-neighbor distance ~~of myelinated axons in SLF~~ was only 6.3 µm but 33 µm for the BDA labeled axons suggesting that only one in five axons was BDA labeled. Myelinated axons ~~(10921 axons were measured as preliminary work for another study)~~ were also significantly thicker (1.3 µm on average) than the BDA labeled axons. This is not surprising since at the locations measured SLF I contain also axons originating in area 4 and elsewhere (see Schmahamann and Pandya, 2009).

Descending Projections from Areas 4 and 9

Axons were sampled at four locations: i) at their entrance into the dorsal aspect of the caudate, ii) in the proximal part of the internal capsule, dorsal to the entrance into the thalamus, iii) at entrance into the thalamus, in proximity to their principal thalamic nuclei, i.e. VL and MD, where a few retrogradely labeled neurons were also seen, and iv) in the distal part of the internal capsule. This location corresponded to the entrance into the cerebral peduncle for the axons from area 4; the axons from area 9 were sampled more dorsally just ventral to the thalamus while coursing towards the *zona incerta*, since the axons reaching the cerebral peduncle were few and difficult to separate from those labeled by the more caudal injection in area 4. In addition, in one experiment, the main tract streaming from the injection site was sampled, i.e. the axons dorsal to the separation of axons directed to the corpus callosum, to the internal capsule and to the caudate (Fig. 5).

To test the consistency of measurements across studies we re-sampled axons to the proximal internal capsule and the results (Table 2 and Fig. 6) well correspond to those of earlier measurements (Tomasi et al. 2012). The mean value of axon diameters from area 4 to the proximal internal capsule is 0.74 and 0.91 µm (medians 0.6 and 0.7 µm) in the two experiments compared to the 0.68 and 1.01 µm (medians 0.59 and 0.89 µm) of the previous estimates in the same animals (Tomasi et al. 2012). For area 9 we found an average diameter of 0.59 µm (median 0.50) vs. 0.51 (mean; 0.46 median) of the previous estimates. Although the results are consistent, in spite of the different methodologies and sampling strategies used, in the two studies, tThe small differences might suggest the existence of local heterogeneities in the axonal composition of the various projections, which further studies might document.

The axons originating from motor cortex area 4 and directed to the thalamic nucleus VL are significantly thicker than those originating from prefrontal cortex area 9 and directed to the

nucleus MD (0.63 and 0.69, in two experiments vs. 0.44 µm; P<0.001). The difference in favor

of area 4 is even larger for axons directed to the distal internal capsule (1.4 and 1.37 vs. 0.54 µm;

P<0.001). Differences in the projection from areas 4 and 9 to the caudate (0.4 and 0.49 vs. 0.36

µm) and to the proximal internal capsule (0.74 and 0.91 vs. 0.59 µm) were just below the

significance level (P<0.05) in one experiment, but were significant in the other.

In conclusion, motor cortex area 4 sends the thickest axons towards the cerebral peduncle

(distal internal capsule) (1.4 and 1.37 µm in the two experiments), thinnest axons to the caudate

nucleus (0.4 and 0.49 µm) while the thalamic nucleus VL receives axons between those two

(0.63 and 0.69 µm). These differences are statistically significant at the 0.05-0.001 level.

The distribution of different diameter axons to different targets could be implemented in

two different ways i.e., collateralization of the axons or parallel axonal systems. ~~Figure 7~~

~~illustrates what the two hypotheses predict.~~ Collateralization predicts that the axons within a tract

would become thinner in the proximal to distal direction while the parallel projection hypothesis

allows for thicker axons distally (Fig. 7). The results of the present measurements are clearly in

favor of the second possibility. Indeed, ~~This is further illustrated in Fig. 8 which shows that~~ the

projection from area 4 (Fig. 8) contains progressively thicker axons in the proximal to distal

direction, while the contingent of thin axon progressively decreases, consistent with the

hypothesis that these axons have terminated at their proximal targets, caudate and thalamus, in

particular.

Consequences for Conduction Velocities and Delays

From the estimated diameters we calculated the conduction velocities and from the length of the

pathways the approximate delay to the target (Table 3 and Fig. 9). Velocity (V) was computed as

previous~~ly~~ ~~publications~~ (Tettoni et al. 1998; Caminiti et al. 2009; Tomasi et al. 2012) as V=(5.5/0.7)*diameter. As confirmed above the factor 0.7 is the average axoplasm-to-myelin ratio and it corrects for the fact that BDA visualizes only the axoplasm, without percolating into the myelin sheath.

The median axon diameter from area PEc to area 4 being 0.8 µm in diameter, it is expected to conduct at approximately 6.3 m/s. The distance (D) from the injection to the site where the diameters were sampled ~~was measured as a single curvilinear segment with one of the Neuroexplorer software options (MBF Biosciences, Williston, VT) and~~ was found to be of approximately 12 mm. The delay to target (T= D/V) ~~can be expected to~~ should be in the order of 1.9 ms. The projection to area 24, being 0.73 µm in diameter ~~it~~ is expected to conduct at 5.7 m/s ~~and the~~ over a distance ~~to the sites of axonal measurements being approximately~~ of 20.2 mm generating ~~the~~ delays ~~to target is expected to be~~ in the order of 3.5 ms. The median axon to area 6 being 0.87 µm in diameter its conduction velocity 6.8 m/s and the path to target approximately 23 mm the delay to target can be expected to be 3.3 ms. Therefore it appears that the information from area PEc should reach area 4 in advance of area 24 or 6.

The conduction velocity from area 4 to VL was 3.9 and 5.5 m/s in CCT 2 and CCT 5, respectively generating delays of 5 and 3.7 ms over conduction distances of 19.6 and 20.3 mm. In contrast the conduction velocity from area 9 to MD was 3.1 m/s, generating delays of 8.3 ms. These findings confirm ~~the previous estimates~~ that delays to their principal thalamic nuclei is greater for prefrontal than motor projections (Tomasi et al. 2012). The estimated conduction velocities to the caudate turned out to be the similar in all experiments (3.1 m/s). The estimated conduction delays ranged between 3.4 and 4.3 ms.

Finally considerable differences in the conduction velocities of axons to the distal internal capsule were found between axons originating in area 4 (7.9 and 9.5 m/s in the two experiments) vs. those originating in area 9 (3.5 m/s). It should be stressed that the conduction delays are rough estimates since axons de-fasciculate near their targets; ~~and therefore~~ more precise estimates ~~amenable to rigorous statistical evaluations~~ would require the serial reconstruction of individual axons to their sites of termination, which was impossible on the present material.

Discussion

Goals and Methodological Considerations

In this study as in previous ones (Caminiti et al. 2009; Tomasi et al. 2012) we have chosen to undertake a light microscopic analysis of axonal projections originating in the cerebral cortex of the macaque monkey with focus on axon diameters and length of the projections. This work has three long-term goals. One is to explore cortical connectivity at the cellular resolution, when this is missing in the current database of brain structure. The second is to allow predictions on the conduction velocity and timing of interaction between the different structures connected to the cerebral cortex, which is relevant for the speed of information processing in the brain and for cortical dynamics (Roxin et al. 2005; Roberts and Robinson, 2008; Caminiti et al. 2009; Panzeri et al. 2010). The third is to allow translation from the structure of the monkey brain to that of the human and/or of other primates in view of applications to human misconnectivity syndromes and to the evolution of the primate brain (Caminiti et al. 2009; Caminiti et al. 2010). Comparisons of cellular monkey data to the human are timely since non-invasive imaging techniques are

approaching the level of resolution required to analyze the axonal diameters in fiber tracts (e.g.

Barazany et al. 2009; Dyrby et al. 2012).

The LM analysis is bound to miss axons with diameters below the level of optical

resolution i.e., 0.2-0.3 µm but it appears to be the only approach possible, in view of the

difficulty of performing systematic EM analyses of labeled axons in primates, particularly in

humans, and in protected primate species. The error intrinsic to the LM analysis of the monkey

material can be estimated by comparison with EM data in the literature when they exist (e.g. the

corpus callosum; discussed in Tomasi et al. 2012). For reasons explained above (Results) we

have chosen to EM-examine the diameter of intracortical axons in the parietal cortex. Our EM

measurements were in the order of the previous LM estimates of intracortical axon diameters

suggesting, as previously proposed (Tomasi et al. 2011), that "the structure of the cortical

modules "columns" or "cortical output units" is invariant across areas because they perform

similar computations" while the computations performed by long projections, and hence their

structure, varies across areas.

Comparison with Previous Studies

The cortico-cortical projections from area PEc resemble those documented in case 3 of

Schmahamann and Pandya (2009). They described projections to area 4 and 6 as well as a

projection to the bottom of the cingulate sulcus in their sections 81-89. Unfortunately our

material did not extend further and therefore we could not analyze the more rostral sites of

termination. As mentioned (Results) our site of termination near the bottom of the cingulate

sulcus has distinct cytoarchitectonic features from the more dorsal part of area 6, which are most

evident in layers 3 and 5, particularly in the pattern of myelination and it appears to correspond to a subdivision of area 24.

Our injection sites in area 4 resemble the more lateral injection of case 1 of Kultas-Ilinsky et al. (2003) and case 27 of Schmahamann and Pandya (2009) but are somewhat smaller and more medial than the latter. The trajectory and location of the descending projection is similar to that documented in the second study. In Kultas-Ilinsky et al. study (2003) the projection was studied within the thalamic nuclei themselves and in ours at the entrance into the thalamus, to measure axonal trunks rather than collaterals. The two studies agree that the projection to the VL overwhelmingly consists of "small" axons, which in their case, distributed small terminal boutons in the order of 0.21-0.6 μm^2 occasionally larger. In addition they found large axons projecting to other thalamic nuclei. These axons might have contributed to our previous sample of the projection to the VL (Tomasi et al. 2012) which consisted of slightly thicker axons. It should be mentioned that Differences in the diameter of axons directed to different thalamic nuclei might be a general feature of cortical projections, across systems and species (e.g. Rockland 1994; Rouiller and Welker 2000; Cappe et al. 2007). The two types of axons might originate from different layers, with thick axons mainly from layer 5 and thin ones from layer 6 as discussed by Kultas-Ilinsky et al. (2003). The projection from area 4 included large axons directed to the cerebral peduncle.

Our conclusion that the projection from area 4 to the thalamus, to the caudate, and to the cerebral peduncle consists mainly or exclusively of different axonal systems seems consistent with the data in the literature which instead reports higher degree of collateralization for descending projections in the brain stem (Lemon 2008). The projection to the thalamus originates mainly from layer 6, while that to the cerebral peduncle and to the striatum is mainly

from layer 5, presumably, in primates, from different neuronal populations. This conclusion is tentative since our work cannot exclude the possibility that, as in the rat, a small population of small or medium size axons may send collaterals to multiple targets including the striatum, thalamus and to the subthalamic nucleus (Kita and Kita, 2012).

Our injection in area 9 is more medially located than that of case 31 of Schmahamann and Pandya (2009) but the axonal trajectories are similar, i.e., to the dorsal aspect of the caudate, to the thalamic nucleus MD , and to the *zona incerta* where we sampled and measured axons.

The finding that axons from area 4 projecting to the cerebral peduncle conduct much faster than those to the caudate is compatible with the electrophysiological evidence that axons to the pyramidal tract are faster than those to another compartment of the basal ganglia, the putamen (Bauswein et al. 1989). However the distribution of axons diameters in the cerebral peduncle (Fig. 8) did not provide the clear bimodal distribution of fast and slow axons, expected from the classical electrophysiological work on the pyramidal tract. Furthermore only 23 of 185 axons measured in two experiments had diameters equal or greater than those compatible with velocities of 25 m/s, which is the cut off proposed by Humphrey and Corrie (1978) between the two populations. This is far from the 45% found by the same authors electrophysiologically with antidromic activation. ~~Also, only one of our axons might have conducted faster than 35 m/s.~~ Humphrey and Corrie (1978) attributed the discordance between their electrophysiological findings and the anatomical data available at the time to a strong electrophysiological sampling bias in favor of large cell bodies. The correction they proposed does indeed provide a better match between their electrophysiological data and our estimates of conduction velocities computed from diameters (Suppl Fig. 1) although our sample still misses axons which could conduct at above 35 m/s. Perhaps thicker axons originate from ~~It is possible that we would have~~

~~found larger axons had a~~ portions of area 4 corresponding to the distal extremity representation ~~been injected~~than in the proximal limb/trunk area we injected. Alternatively, the axons we measured might have shrunken, due to the fixation and histological processing. The correction for shrinkage we applied (Methods) returned slightly higher conduction velocities (Suppl Fig.2), but the results are still far from the electrophysiological data. The electrophysiological bias remains the most likely explanation of the discrepancy of data although in a previous paper (Tomasi et al. 2012) we found that conduction velocities and latencies predicted from the anatomical data (uncorrected for shrinkage) of interhemispheric connections of peristriate areas perfectly matched those found in an electrophysiological study of antidromic responses.

Consequences and determinants of axon diameters

Confirming and extending previous results (Caminiti et al. 2009; Tomasi et al. 2012) we found that axons of different caliber originate from different areas. The comparison of projections issued from area 4 and 9, chosen because they represent the extremes in the spectrum of outgoing-axon diameters, showed thinner axons from area 9 to the thalamus and internal capsule, in addition to the corpus callosum (Caminiti et al. 2009; Tomasi et al. 2012). Interestingly this appears not to apply to the projections to the caudate which receives similarly thin axons from the two areas nor to the intra-areal axons.

It remained to be clarified if an area also sends different diameter axons to different targets. The finding that parietal cortex projects thinner cortico-cortical axons to area 24 than to area 4 and 6 and the analysis of comparable projections in the two animals injected in the motor cortex area 4 indicate unequivocally that they do. Moreover it appears that axons with different

diameter originate from different neuronal populations and proceed in parallel to the different targets.

The relations between origin and termination of cortical axons and their diameters highlight what appear to be new aspects of cortical organization. Together they suggest that the overall picture which should arise from systematic studies of this kind is one of an extraordinary complexity of axonal pathways operating at different conduction speed and generating different conduction delays between brain sites. The complexity is exaggerated by the finding that each projection consists of axons with different diameter, which therefore cause a spectrum of activation delays at their targets. In the evolution of primates the diameter of axons increases less than the distance between sites caused by brain enlargement and the spectrum of delays increased as well with probable consequences for brain dynamics (Caminiti et al. 2009). An additional question is whether feed-forward and feed-back projections between two areas use similar spectra of axon diameters and conduction velocities as this appears to be the case for the V1-V2 projections in the monkey (Girard et al., 2001).

Which could be the consequences of the different conduction properties of cortical axons? One might be the existence of a hierarchical organization of cortical areas in terms of processing speed, the primacy going to the premotor, motor and somatosensory systems (Tomasi et al. 2012). Unfortunately, at least three crucial pieces of information are missing. One is that the axon diameters are roughly proportional to size of the parent somata (Tomasi et al. 2012), which might have different activation threshold and this could compensate for the delays generated by the axons. The second is that different diameter axons might contact different types of neurons. For example, it was suggested that inhibitory influences between the hemispheres might be carried by faster axons (Makarov et al. 2008) although the slower interhemispheric

input may be overwhelmingly excitatory (Makarov et al. 2008; Wunderle et al. 2012). The third unknown concerns the conduction and synaptic properties of the intracortical, terminal portion of the axons and the dynamics of the neuronal compartments they impinge. This includes the neuronal integration time, discussed by Budd and Kisvarday (2012).

A different set of questions, which will be only briefly mentioned here, relates to the mechanisms which control axon diameter. In development, large axon diameters progressively differentiate from an initially uniform or almost uniform distribution of small axons (Berbel et al. 1988; LaMantia and Rakic 1990). What causes this differentiation? Area-of-origin axonal signatures appear to be a new aspect of cortical regionalization and an additional, possibly genetically determined feature of cortical areas. The search for area specific genes has proven to be a difficult task, particularly in primates (Yamamori et. al. 2006; Molnar and Clowry 2012) although promising perspectives emerge from complex layer- and area-specific gene clustering analyses (Bernard et al. 2012) and from the study of the differences in the transcriptional activity of certain genes (Konopka et al. 2012). Axonal differences related to the site of termination are probably the expression of the genotypic identity of cortical projection neurons (e.g. Leone et al. 2008; Molyneaux et al. 2007; Shim et al. 2012), but also of possible retrograde signals from the target. Beyond the likely genetic predisposition neural activity certainly plays a role as shown by the catastrophic consequences of interfering with activity on the development of callosal projections (reviewed in Innocenti 2007; see also Wang et al. 2007).

The cellular mechanisms of axonal radial growth are incompletely known. Cytoskeletal components the neurofilaments, in particular their heavy subunit, but also the intermediate molecular weight subunit are involved in axonal maturation (Figlewicz et al. 1988) and radial growth (Rao et al. 2003; Perrot et al. 2007 and references therein). It was long believed that all

the axonal proteins are synthetized in the cell body but now unequivocal evidence of axonal translation has accumulated (Keonig et al. 1967; Giuditta et al. 1968; reviewed in Jung et al. 2012) although thus far evidence that the cytoskeletal proteins are also axonally synthetized is lacking. A key element in the regulation of axonal caliber is the oligodendrocyte as shown by the finding that axons fail to grow at sites where oligodendrocytes have been deleted by irradiation (Colello et al. 1994). Some of the molecular mechanisms of the oligodendrocytic action on the axon have been discovered recently (Lee et al. 2012). Oligodendrocyte proliferation is in turn regulated by a host of factors, including the already mentioned neurofilament proteins proteins (Fressinaud et al. 2012). Obviously the reciprocal interactions between axons, axonal cytoskeleton, olygodendrocytes and neural activity remain elusive.

It would be important to know how the many complex cellular and molecular events which determine axon diameters and the conduction delays are coordinated and regulated over the whole brain, in development and possibly in adulthood. The counterpart of this question is what the consequences of deregulation might be, a possible cause for misconnectivity syndromes, including schizophrenia (Innocenti et al. 2003) resulting in psychiatric and/or neurological symptoms.

TABLES

	SLF	to area 4	to area 24	to area 6
Mean	1.03	0.95	0.77	0.96
Median	0.80	0.80	0.73	0.87
Mode	0.51	0.44	0.66	0.58
St Deviation	0.75	0.57	0.21	0.36
Sample Variance	0.56	0.33	0.05	0.13
Kurtosis	4.87	5.86	2.10	2.03
Skewness	2.09	2.04	1.40	1.21
Range	4.16	3.50	1.16	1.97
Minimum	0.29	0.29	0.44	0.44
Maximum	4.45	3.79	1.60	2.41
Count	273	207	203	164

Table 1 Axons from area PEc projecting to other cortical areas.

Motor Area 4 (µm)

CCT 2	to caudatus	to ic prox	to thalamus	to ic dist
Mean	**0.40**	**0.74**	**0.63**	**1.40**
Median	**0.40**	**0.60**	**0.50**	**1.20**
Mode	0.40	0.40	0.40	1.60
St Deviation	0.19	0.54	0.33	0.85
Sample Variance	0.04	0.29	0.11	0.73
Kurtosis	15.55	6.75	2.43	0.70
Skewness	3.51	2.23	1.38	0.99
Range	1.20	3.20	1.80	3.50
Minimum	0.20	0.20	0.20	0.30
Maximum	1.40	3.40	2.00	3.80
Count	80	87	80	84

CCT 5	main tract	to caudatus	to ic prox	to thalamus	to ic dist
Mean	**0.79**	**0.49**	**0.91**	**0.69**	**1.37**
Median	**0.50**	**0.40**	**0.70**	**0.70**	**1.00**
Mode	0.30	0.40	0.40	0.40	1.20
St Deviation	0.67	0.25	0.66	0.32	1.10
Sample Variance	0.45	0.06	0.44	0.10	1.21
Kurtosis	4.18	5.67	15.90	0.87	5.86
Skewness	1.81	2.07	3.06	1.01	2.11
Range	3.70	1.50	5.00	1.50	6.60
Minimum	0.20	0.20	0.20	0.30	0.20
Maximum	3.90	1.70	5.20	1.80	6.80
Count	105	119	108	104	101

Prefrontal Area 9 µm

CCT 2	to caudatus	to ic prox	to thalamus	to ic dist
Mean	**0.36**	**0.59**	**0.44**	**0.54**
Median	**0.40**	**0.50**	**0.40**	**0.45**
Mode	0.40	0.40	0.40	0.40
StDeviation	0.11	0.25	0.13	0.27
Sample Variance	0.01	0.06	0.02	0.07
Kurtosis	2.22	1.21	5.16	3.50
Skewness	0.62	1.14	1.95	1.64
Range	0.60	1.20	0.80	1.40
Minimum	0.10	0.30	0.20	0.20
Maximum	0.70	1.50	1.00	1.60
Count	80.00	103.00	100.00	100.00

Table 2 Size of axons originating from different injection sites and projecting to n. caudatus,

internal capsule and to the thalamus.

Cortico-cortical axons

	diameter median μm	velocity m/s	path μm	delay μs
PEc to a 4	0.8	6.29	12041	1916
PEc to a 24	0.73	5.74	20201	3522
PEc to a 6	0.87	6.84	23001	3365

Descending axons

	diameter median μm	velocity m/s	path μm	delay μs
CCT2 area 9 to MD	0.4	3.14	25934	8252
CCT2 area 4 to VL	0.5	3.93	19615	4993
CCT5 area 4 to VL	0.7	5.50	20306	3692
CCT2 area 9 to caudate	0.4	3.14	10586	3368
CCT2 area 4 to caudate	0.4	3.14	13475	4288
CCT5 area 4 to caudate	0.4	3.14	12293	3911
CCT2 area 9 to distal ic	0.45	3.54		
CCT2 area 4 to distal ic	1.2	9.43		
CCT5 area 4 to distal ic	1	7.86		

Table 3 Conduction velocities path lengths and delays

CAPTIONS TO FIGURES

Figure 1. Location and extent of BDA injection sites. Top: area PEc injection in experiment CCT1; middle: area 9 injection in CCT2; bottom: area 4 injection in CCT5. Each injection site is shown in outlines of the section and in photomicrographs of BDA-reacted material. Vertical segments mark the boundaries of area PEc close to the border with PE (top panel), 9L and 46 (and the 9/46 transition between the two, not labeled; middle panel) and area 4 (bottom panel); the outlines of the injection site are also projected on the CV stained section were the large pyramids of layer 5 can be appreciated and the injection track is marked by an arrow. Calibration bars are 1 mm in the section outlines and 500 µm in the photomicrographs.

Figure 2. Photomicrographs of three myelinated (A, B, D) and one unmyelinated (C), BDA labeled axons. Calibration bars are 0.5 µm.

Figure 3. Location of axon measurement sites (white polygons) in the SLF (bottom panel), and at the entrance of axons in area 4 (top left), areas 24 and 6 (top right) along the sketched axonal pathways in superposed outlines of sequential, non-consecutive, sections. Calibration bars are 2000 µm.

Figure 4. Bar diagram of axon diameters at different locations long the parieto-frontal projection. S35 denotes the section where measurements were performed.

Figure 5. Location of axon measurement sites (white polygons) at different locations in the projection from area 4, along the sketched axonal pathways in superposed outlines of sequential, non-consecutive, sections (experiment CCT2). Insets show axonal labeling and selection of axonal segments at the entrance into caudate and traced axons in proximal internal capsule in experiment CCT5.

Figure 6. Bar diagram of mean axon diameters (and standard deviations) at different locations in the projections from areas 4 and 9.

Figure 7. The collateralization and parallel pathway hypotheses and their predictions.

Figure 8. Axon diameter distributions show a progressive proximo-distal shift towards thicker axons and disappearance of thinner axons compatible the parallel pathway hypothesis (Fig. 7).

Figure 9. Schematic representation of diameters and estimated conduction delays for the connections studied, in this paper and in Tomasi et al. (2012). Thickness of arrow segments is proportional to median diameter; projections from area 4 are the means of two animals. Delays are calculated on conduction velocities and pathway lengths (Table 3). Delays computed in the same animal are shown in different colors i.e. CCT1: black, CCT2: red, CCT5: blue. Filled boxes are areas studied in the present paper. Open boxes are from Tomasi et al (2012); ptem and mtem refer to posterior and middle temporal areas.

REFERENCES

Barazany D, Basser PJ, Assaf Y. 2009. In vivo measurement of axon diameter distribution in the corpus callosum of rat brain. Brain. 132:1210-1220.

Bauswein E, Fromm C, Preuss A. 1989. Corticostriatal cells in comparison with pyramidal tract neurons: contrasting properties in the behaving monkey. Brain Res. 493:198-203.

Belmalih A, Borra E, Contini M, Gerbella M, Rozzi S , Luppino G. 2007. A multiarchitectonic approach for the definition of functionally distinct areas and domains in the monkey frontal lobe. J Anat. 211:199-211.

Berbel P, Innocenti GM. 1988. The development of the corpus callosum in the cat. A light- and electron-microscopic study. J Comp Neurol. 276:132-156.

Bernard A, Lubbers LS, Keith Q, Tanis KQ, Luo R, Podtelezhnikov AA, Finney EM, McWhorter MME, Serikawa K, Lemon T, Morgan R, Copeland C, Smith K, Cullen V, Davis-Turak J, Lee C-K, Sunkin SM, Loboda AP, Levine DM, Stone DJ, Hawrylycz MJ, Roberts CJ, Jones AR, Geschwind DH, Lein ES. 2012. Transcriptional Architecture of the Primate Neocortex. Neuron. 73:1083-1099.

Budd JML, Kisvarday ZF. 2012. Communication and wiring in the cortical connectome. Front Neuroanat. 6:1-23.

Caminiti R, Ghaziri H, Galuske R, Hof PR, Innocenti GM. 2009. Evolution amplified processing with temporally dispersed, slow neuronal connectivity in primates. Proc Natl Acad Sci USA. 106:19551-19556.

Caminiti R, Chafee MV, Battaglia-Mayer A, Averbeck B, Crowe DA, Georgopoulos AP. 2010. Understanding the parietal lobe syndrome from a neurophysiological and evolutionary perspective. Eur J Neurosci. 31:2320–2340.

Cappe C, Morel A, Rouiller EM. 2007. Thalamocortical and the dual pattern of corticothalamic projections of the posterior parietal cortex in macaque monkeys. Neuroscience. 146:1371-1387.

Colello RJ, Pott U, Schwab ME. 1994. The role of oligodendrocytes and myelin on axon maturation in the developing rat retinofugal pathway. J Neurosci. 1994. 14:2594-2605.

Dyrby TB, Søgaard LV, Hall MG, Ptito M, Alexander DC. 2012. Contrast and stability of the axon diameter index from microstructure imaging with diffusion MRI. Magn Reson Med. 2012 Sep 28. [Epub ahead of print].

Figlewicz DA, Gremo F, Innocenti GM. 1988. Differential expression of neurofilament subunits in the developing corpus callosum. Dev Brain Res. 42:181-189.

Fressinaud C, Berges R, Eyer J. 2012. Axon cytoskeleton proteins specifically modulate oligodendrocyte growth and differentiation in vitro. Neurochem Int. 60:78–90.

Girard P, Hupé JM, Bullier J. 2001. Feedforward and feedback connections between areas V1 and V2 of the monkey have similar rapid conduction velocities J Neurophysiol. 85:1328-1331.

Giuditta A, Dettbarn WD, Brzin M. 1968. Protein synthesis in the isolated giant axon of the squid. Proc Natl Acad Sci USA. 59:1284–1287.

Humphrey Dr, Corrie WS. 1978. Properties of pyramidal tract neuron system within a functionally defined subregion of primate motor cortex. J Neurophysiol. 41:216-243.

Innocenti GM. 2007. Subcortical regulation of cortical development. Some effects of early cortical deprivation. In Von Hofsten C, Rosander K (Eds) Progr Brain Res. 164:23-37.

Innocenti GM, Ansermet F, Parnas J. 2003. Schizophrenia, development and corpus callosum. Molec Psychiat. 8:261-274.

Jung H, Yoon BC, Holt CE. 2012. Axonal mRNA localization and local protein synthesis in nervous system assembly, maintenance and repair. Nature Rev Neurosci. 13:308-324.

Koenig E. 1967. Synthetic mechanisms in the axon. IV. In vitro incorporation of [3H]precursors into axonal protein and RNA. J Neurochem. 14:437–446.

Konopka G, Friedrich T, Davis-Turak J, Winden K, Oldham MC, Gao F, Chen L, Wang GZ, Luo R, Preuss TM, Geschwind DH. 2012. Human-specific transcriptional networks in the brain. Neuron. 75:601-17.

Kultas-Ilinski K, Sivan-Loukianova E, Ilinski IA. 2003. Reevaluation of the Primary Motor Cortex Connections with the Thalamus in Primates. J Comp Neurol. 457:133–158.

LaMantia AS, Rakic P. 1990. Cytological and quantitative characteristics of four cerebral commissures in the rhesus monkey. J Comp Neurol. 291:520-537.

Lee Y, Morrison BM, Li Y, Lengacher S, Farah MH, Hoffman PN, Liu Y, Tsingalia A, Jin L, Zhang PW, Pellerin L, Magistretti PJ, Rothstein JD. 2012. Oligodendroglia metabolically support axons and contribute to neurodegeneration. Nature. 487:443-448.

Lemon RN. 2008. Descending Pathways in Motor Control. Annu Rev Neurosci. 31:195–218.

Leone DP, Srinivasan K, Chen B, Alcamo E, McConnell SK. 2008. The determination of projection neuron identity in the developing cerebral cortex. Curr Opin Neurobiol. 18:28-35.

Makarov VA, Schmidt K, Castellanos NP, Aguado L, Innocenti GM. 2008. Stimulus–dependent interactions between the visual areas 17 and 18 of the ferret. Cereb Cortex, 18:1951-1960.

Molnár Z, Clowry G. 2012. Cerebral cortical development in rodents and primates M. A. In Hofman MA, Falk D (Eds.) Progr Brain Res. 195:45-70.

Molyneaux BJ, Arlotta P, Menezes JR, Macklis JD. 2007. Neuronal subtype specification in the cerebral cortex. Nat Rev Neurosci. 8:427–437.

Panzeri S, Brunel N, Logothetis NK, Kayser C. 2010. Sensory neural codes using multiplexed temporal scales. Trends Neurosci. 33:111-120.

Paxinos G, Huang X-F, Toga AW. 2000. The Rhesus Monkey Brain. London: Academic Press.

Perrot R, Lonchampt P, Peterson AC, Eyer J. 2007. Axonal neurofilaments control multiple fiber properties but do not influence structure or spacing of nodes of Ranvier. J Neurosci. 27:9573–9584.

Picard N, Strick PL. 1996. Motor areas of the medial wall: a review of their location and functional activation. Cerebr Cortex. 6:342-353.

Rao MV, Campbell J, Yuan A, Kumar A, Gotow T, Uchiyama Y, Nixon RA. 2003. The neurofilament middle molecular mass subunit carboxyl-terminal tail domains is essential for the radial growth and cytoskeletal architecture of axons but not for regulating neurofilament transport rate. J Cell Biol. 163:1021-1031.

Roberts JA, Robinson PA. 2008. Modeling distributed axonal delays in mean-field brain dynamics. Phys Rev E Stat Nonlin Soft Matter Phys.78:051901.

Rockland KS. 1994. Further evidence for two types of corticopulvinar neurons. Neuroreport. 5:1865-1868.

Roxin A, Brunel N, Hansel D. 2005. Role of delays in shaping spatiotemporal dynamics of neuronal activity in large networks. Phys Rev Lett. 94:238103.

Rouiller EM, Welker E. 2000. A comparative analysis of the morphology of corticothalamic projections in mammals. Brain Res Bull. 53:727-734.

Shim S, Kwan KY, Li M, Lefebvre V, Sestan N. 2012. Cis-regulatory control of corticospinal system development and evolution. Nature. 486:74-79.

Schmahamann JD, Pandya DN. 2009. Fiber pathways of the brain. New York: Oxford UP.

Tettoni L, Georghita-Bachler F, Bressoud R, Welker E, Innocenti GM. 1998. Constant and variable aspects of axonal phenotype in cerebral cortex. Cereb Cortex. 8:543-552.

Tomasi S, Caminiti R, Innocenti GM. 2012. Areal differences in diameter and length of corticofugal projections. Cereb Cortex. 22:1463-1472.

Yamamori T, Rockland KS. 2006. Neocortical areas, layers, connections, and gene expression. Neurosci Res. 55:11–27.

Wang CL, Zhang L, Zhou Y, Zhou J, Yang XJ, Duan SM, Xiong ZQ, Ding YQ. 2007. Activity-dependent development of callosal projections in the somatosensory cortex. J Neurosci. 27:11334-11342.

Wang N, Warren S, May PJ. 2010. The macaque midbrain reticular formation sends side-specific feedback to the superior colliculus. Exp Brain Res. 201:701-717.

Wunderle T, Eriksson D, Schmidt KE. 2012. Multiplicative Mechanism of Lateral Interactions Revealed by Controlling Interhemispheric Input. Cereb Cortex. 2012 Apr 2. [Epub ahead of print].

Figure 1. Location and extent of BDA injection sites. Top: area PEc injection in experiment CCT1; middle: area 9 injection in CCT2; bottom: area 4 injection in CCT5. Each injection site is shown in outlines of the section and in photomicrographs of BDA-reacted material. Vertical segments mark the boundaries of area PEc close to the border with PE (top panel), 9L and 46 (and the 9/46 transition between the two, not labeled; middle panel) and area 4 (bottom panel); the outlines of the injection site are also projected on the CV stained section were the large pyramids of layer 5 can be appreciated and the injection track is marked by an arrow. Calibration bars are 1 mm in the section outlines and 500 μm in the photomicrographs.
87x125mm (300 x 300 DPI)
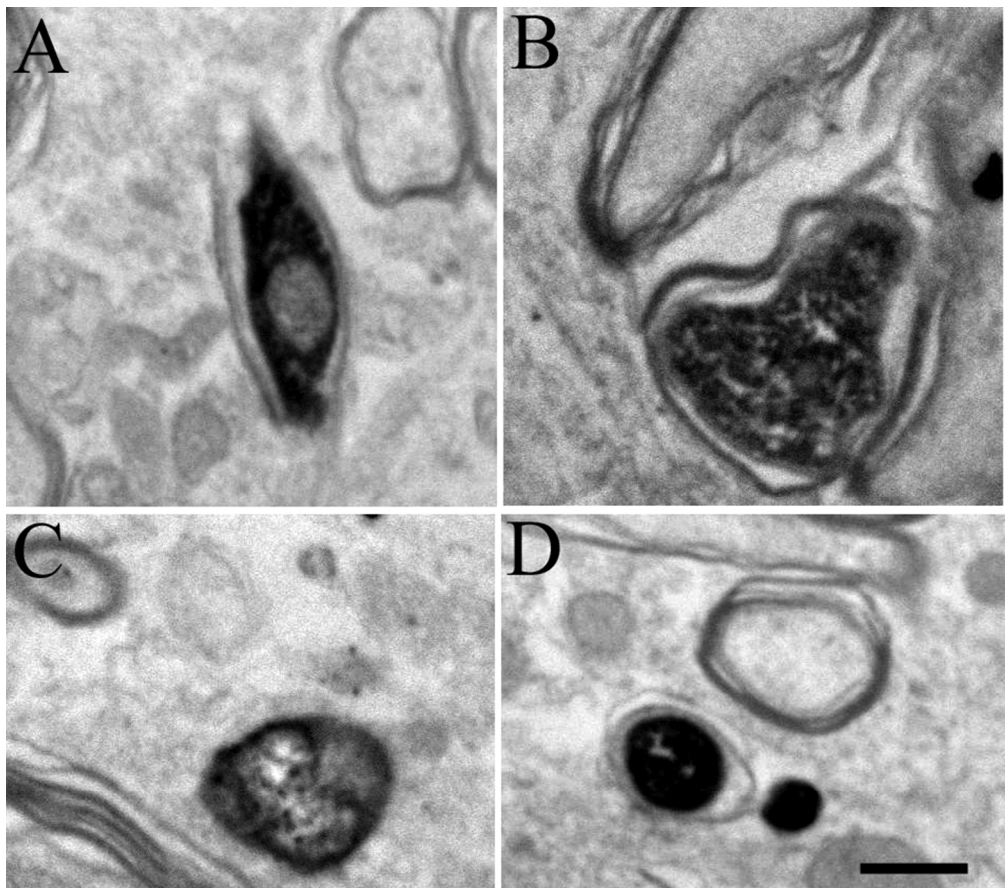
Figure 2. Photomicrographs of three myelinated (A, B, D) and one unmyelinated (C), BDA labeled axons.
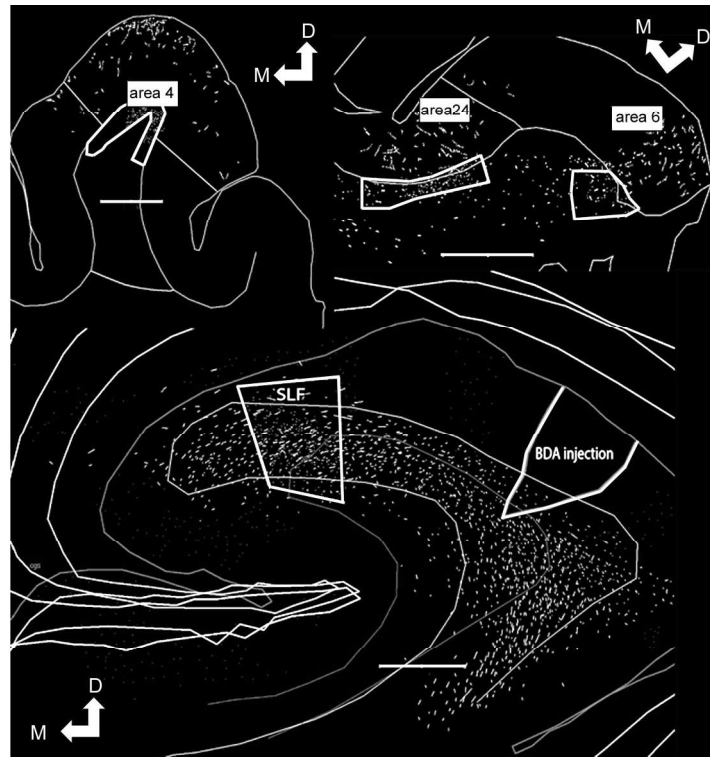Calibration bars are 0.5 µm.
80x70mm (300 x 300 DPI)

Figure 3. Location of axon measurement sites (white polygons) in the SLF (bottom panel), and at the entrance of axons in area 4 (top left), areas 24 and 6 (top right) along the sketched axonal pathways in superposed outlines of sequential, non-consecutive, sections. Calibration bars are 2000 μm.
180x134mm (300 x 300 DPI)
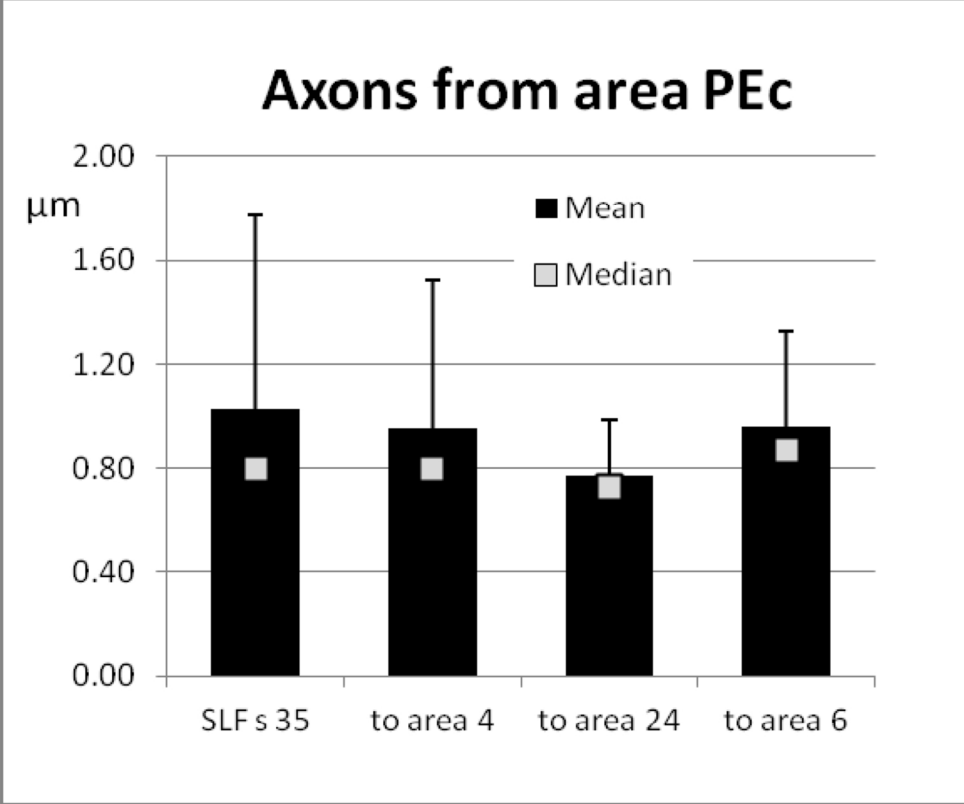
Figure 4. Bar diagram of axon diameters at different locations long the parieto-frontal projection. S35 denotes the section where measurements were performed.
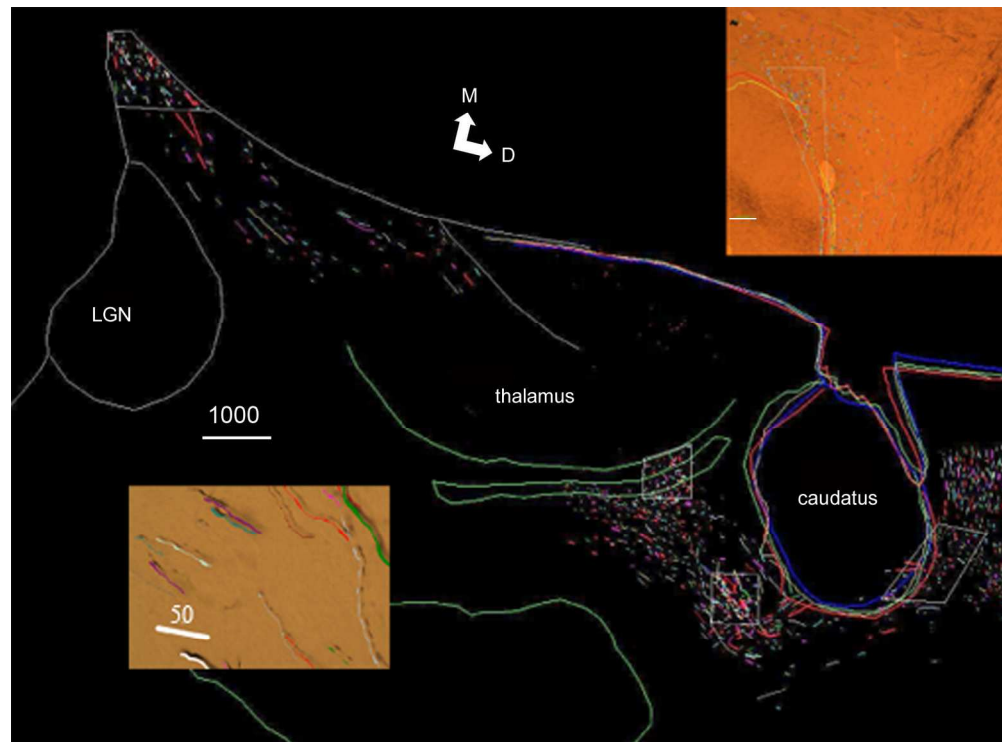66x54mm (600 x 600 DPI)

Figure 5. Location of axon measurement sites (white polygons) at different locations in the projection from area 4, along the sketched axonal pathways in superposed outlines of sequential, non-consecutive, sections (experiment CCT2). Insets show axonal labeling and selection of axonal segments at the entrance into caudate and traced axons in proximal internal capsule in experiment CCT5.
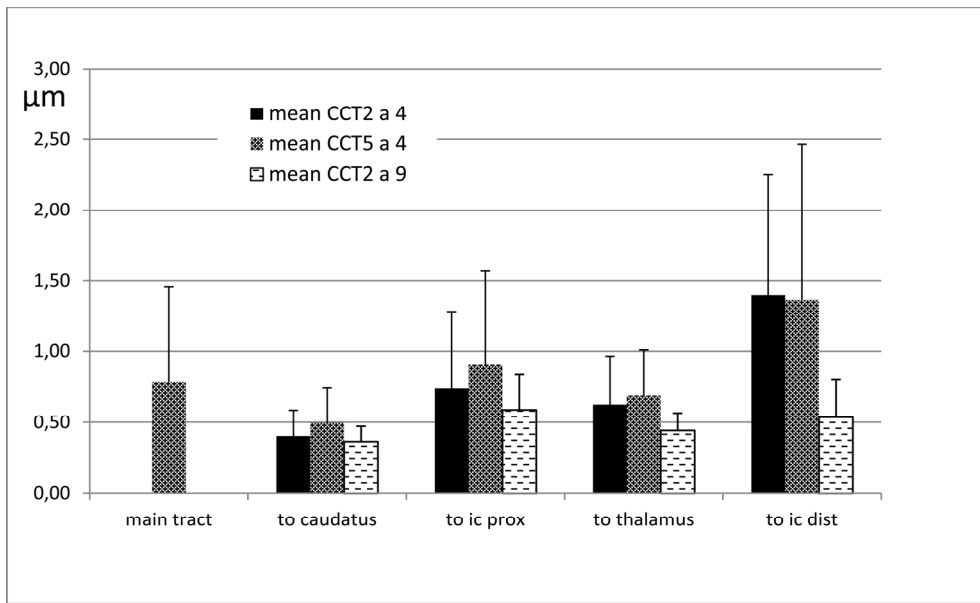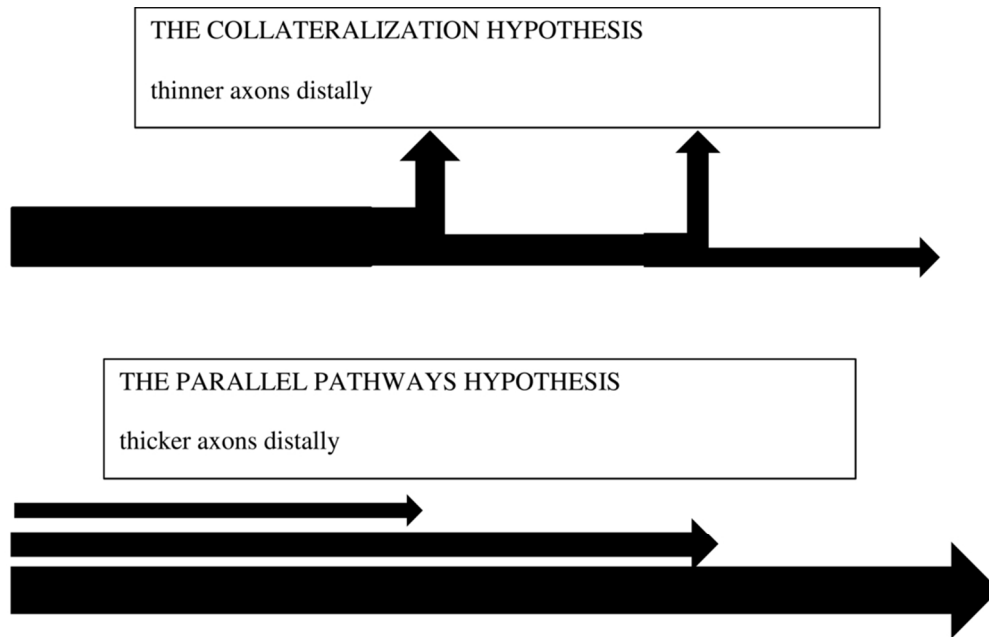
179x132mm (300 x 300 DPI)

Figure 6. Bar diagram of mean axon diameters (and standard deviations) at different locations in the projections from areas 4 and 9.
97x59mm (600 x 600 DPI)

THE COLLATERALIZATION HYPOTHESIS

thinner axons distally

THE PARALLEL PATHWAYS HYPOTHESIS

thicker axons distally

Figure 7. The collateralization and parallel pathway hypotheses and their predictions.
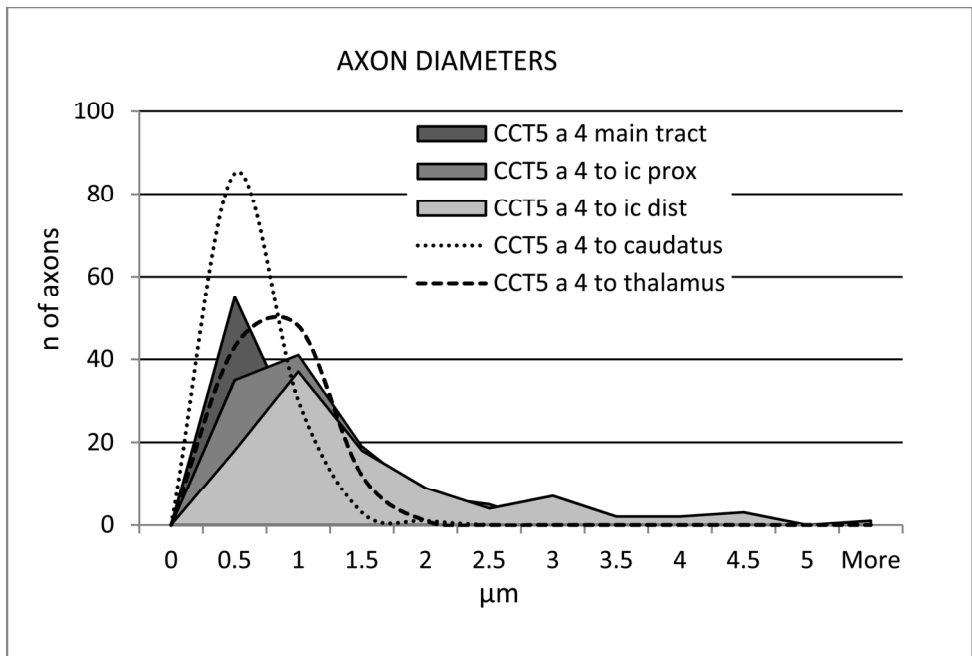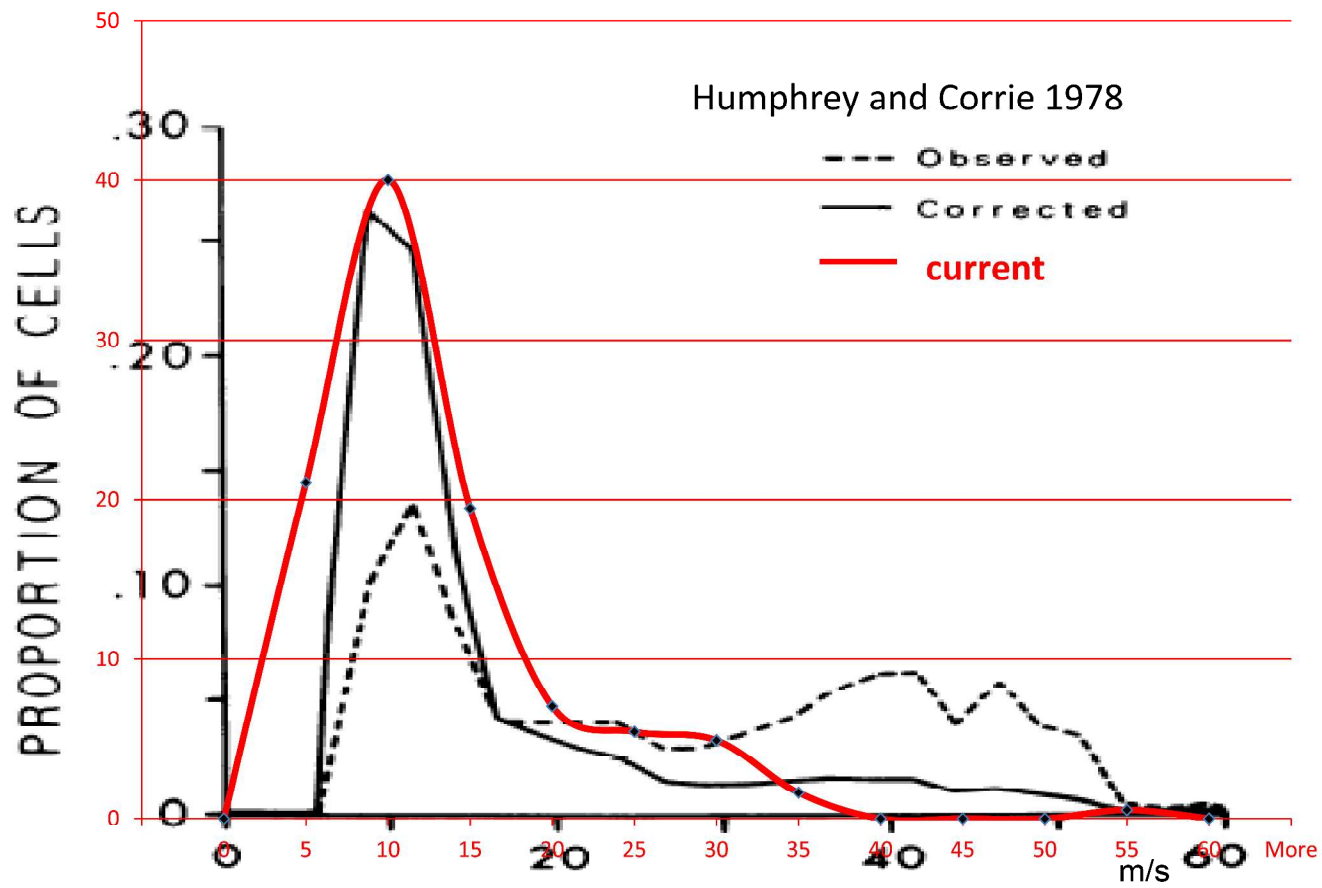50x31mm (600 x 600 DPI)

Figure 8. Axon diameter distributions show a progressive proximo-distal shift towards thicker axons and disappearance of thinner axons compatible the parallel pathway hypothesis (Fig. 7).
87x59mm (600 x 600 DPI)

Figure 9. Schematic representation of diameters and estimated conduction delays for the connections studied, in this paper and in Tomasi et al. (2012). Thickness of arrow segments is proportional to median diameter; projections from area 4 are the means of two animals. Delays are calculated on conduction velocities and pathway lengths (Table 3). Delays computed in the same animal are shown in different colors i.e. CCT1: black, CCT2: red, CCT5: blue. Filled boxes are areas studied in the present paper. Open boxes are from Tomasi et al (2012); ptem and mtem refer to posterior and middle temporal areas.
254x190mm (300 x 300 DPI)

Supplementary Figure 1. Superposition of the spectrum of conduction velocities computed from axon diameters in this study (red histogram) on conduction velocity measurements of Humphrey and Corrie (1978).

	CCT2,CCT5 sum	
Bin	corrected	original
0	0	0
5	24	39
10	52	74
15	43	36
20	30	13
25	11	10
30	11	9
35	4	3
40	6	0
45	3	0
50	0	0
55	0	1
60	0	0
More	1	0
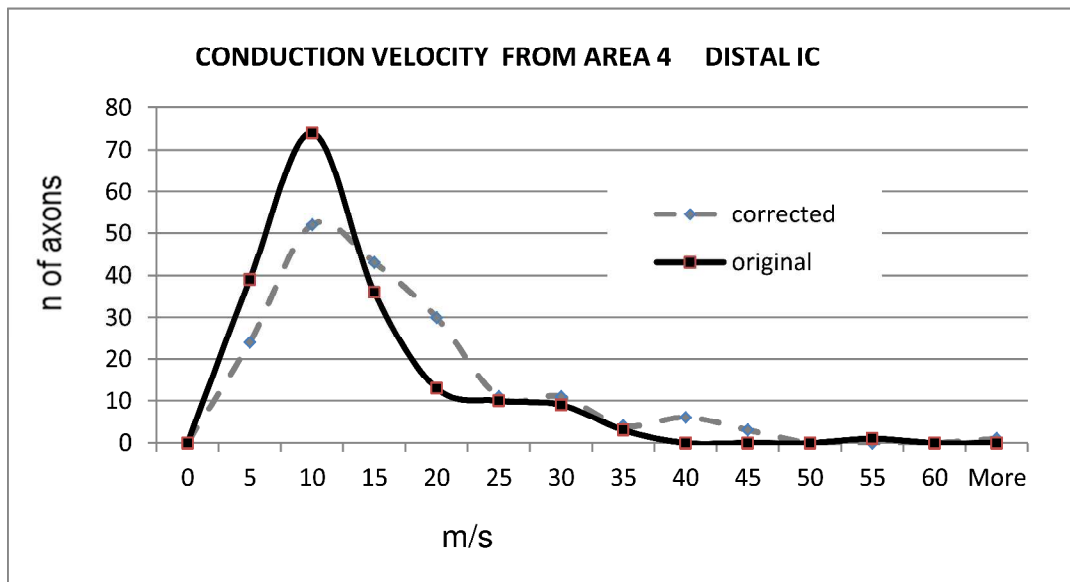
Supplementary Figure 2. Table and histograms of distribution of conduction velocities computed from axonal diameters before and after correction for shrinkage (see text).